Mechanism of Sulfoxide Formation through Reaction of Sulfur Radical Cation Complexes with Superoxide or Hydroxide Ion in Oxygenated Aqueous Solution

Brian L. Miller,[†] Todd D. Williams,[§] and Christian Schöneich*,[†]

Contribution from the Department of Pharmaceutical Chemistry, 2095 Constant Avenue, University of Kansas, Lawrence, Kansas 66047, and Mass Spectrometry Laboratory, University of Kansas, Lawrence, Kansas 66045

Received June 17, 1996[⊗]

Abstract: We have characterized and quantified several pathways which transform aliphatic sulfur radical cations into sulfoxides in aqueous solution. Sulfur radical cations were produced photochemically via one-electron photooxidation through triplet 4-carboxybenzophenone. Sulfur radical cations and superoxide yield sulfoxide, confirmed by oxygen product isotope effects and an inhibitory role of superoxide dismutase. On the basis of competition experiments with superoxide dismutase the rate constant for the reaction between dimethylsulfide radical cations and superoxide was derived as $(2.3 \pm 1.2) \times 10^{11}$ M^{-1} s^{-1}. A demetalated variant of superoxide dismutase did not inhibit superoxide mediated sulfoxide formation, confirming the importance of an active site of the enzyme for inhibition. The stoichiometry of 2 equiv of sulfoxide per reaction of superoxide with a sulfur radical cation suggests a pathway like the singlet oxygen mediated sulfoxide formation, i.e., via a persulfoxide intermediate formed via (i) direct coupling of superoxide with the sulfur radical cation or (ii) electron transfer followed by addition of the product singlet oxygen to a nonoxidized sulfide. In aqueous solution the persulfoxide may add water to yield a hydroperoxy sulfurane prior to its reaction with a second nonoxidized sulfide. At pH values larger than 9, hydroxide ion starts to compete with superoxide for sulfur radical cations and reacts with the persulfoxide or hydroperoxy sulfurane intermediates, initiating less effective pathways of sulfoxide formation. One pathway involves the formation of hydroxysulfuranyl radicals and their reaction with oxygen, supported by product and solvent isotope effects. Besides superoxide and hydroxide-mediated sulfoxide formation there is an additional route involving methylthiomethylperoxyl radicals. Based on oxygen product isotope effects, the latter appear to transfer oxygen onto the sulfide rather than reacting via electron transfer.

Introduction

Organic sulfides serve an important function in many materials such as organic polymers and biological macromolecules. They are highly susceptible to oxidation, and different pathways have been established depending on the nature of the oxidizing species. Potential intermediates have been characterized such as zwitterionic structures, $>^{(+)}$S-O-$O^{(-)}$, available through the addition of singlet oxygen to a thioether.[1,2] Recently, we have identified a mechanism by which aliphatic sulfide radical cations (here from dimethylsulfide, DMS), $>S^{\bullet+}$ (**1a**), and in particular the radical cation complexes $[>S\therefore S<]^+$ (**2a**), can form sulfoxide in oxygen-containing aqueous solution.[3]

$$>S + Ox \rightarrow Ox^{\bullet-} + >S^{\bullet+}\ (\mathbf{1a}) \qquad (1)$$

$$>S + Ox \xrightarrow{>S} Ox^{\bullet-} + [>S\therefore S<]^+ (\mathbf{2a}) \qquad (2)$$

This mechanism is summarized in reactions 1−7, initiated by one-electron oxidation of an aliphatic sulfide (reactions 1 and 2), and completed through hydroxide/water attack on **2a** yielding sulfuranyl radicals of structure **3** or **4**, respectively. These sulfuranyl radicals react with molecular oxygen to yield sulfoxide and superoxide anion. Merényi et al. obtained the overall rate constant for the reaction of **4** with oxygen as $k = 2.0 \times 10^8$ M^{-1} s^{-1} [4] and a relatively stable intermediate **5** can be postulated by analogy to a similar species from the model sulfide 2-(methylthio)methyl acetate ($k_{6,2-(methythio)methyl\ acetate} = 1.1 \times 10^8$ M^{-1} s^{-1}).[5]

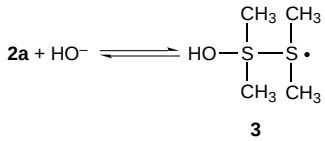

3 (3)

$$\mathbf{2a} + HO^- \rightleftharpoons >S + HO\text{-}S^{\bullet}< (\mathbf{4}) \qquad (4)$$

$$\mathbf{3} + O_2 \rightarrow >S + >S{=}O + H^+ + O_2^{\bullet-} \qquad (5)$$

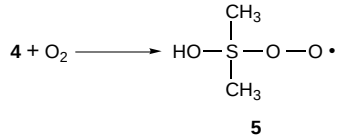

5 (6)

$$\mathbf{5} \rightarrow >S{=}O + H^+ + O_2^{\bullet-} \qquad (7)$$

Apart from reactions 3−7, sulfoxide formation could alternatively proceed via the reaction of superoxide anion with **2a** (reaction 8), in particular under conditions where signifi-

* Correspondence: FAX: (913) 864-5736; email: schoneich@smissman.hbc.ukans.edu.
† Department of Pharmaceutical Chemistry
§ Mass Spectrometry Laboratory.
⊗ Abstract published in *Advance ACS Abstracts,* November 1, 1996.
(1) Jensen, F.; Foote, C. S. *J. Am. Chem. Soc.* **1988**, *110*, 2368−2375.
(2) Akasaka, T.; Yabe, A.; Ando, W. *J. Am. Chem. Soc.* **1987**, *109*, 8085−8087.
(3) Schöneich, Ch.; Aced, A.; Asmus, K.-D. *J. Am. Chem. Soc.* **1993**, *115*, 11376−11383.

S0002-7863(96)02032-X CCC: $12.00

cant concentrations of **2a** and superoxide are generated simultaneously.[6−8]

$$\mathbf{2a} + O_2^{\bullet -} \rightarrow [\text{intermediate(s)}] \quad (\rightarrow \text{sulfoxide} + \text{products}) \tag{8}$$

This process may involve the formation of a zwitterionic intermediate such as formed during the reaction of singlet oxygen with sulfides and, thus, show product stoichiometries comparable to those of singlet oxygen pathways.

Considering these reactions it appears that sulfur radical cations or their dimeric forms are potential key intermediates en route to sulfoxide formation in many chemical and biological systems. This necessitates a detailed understanding of the individual mechanisms underlying sulfoxide formation from sulfur radical cations. In the present study we have quantified and characterized several of these pathways by subjecting aliphatic sulfides to one electron-transfer photooxygenation by triplet 4-carboxybenzophenone (^{3}CBP) in aqueous solution. An emphasis on aliphatic sulfides is particularly important with respect to their model character for biological molecules such as methionine. The existence of reaction 8 was unambigously proven by performing the experiments in the presence of native and des-Cu superoxide dismutase, and corresponding rate constants were derived. Further mechanistic details were obtained on the basis of solvent isotope and product isotope effects.

Results

A. Photolytic Yields of ^{3}CBP and Dimethyl Sulfide Radical Cations in H_2O and D_2O. The photolytic yields of ^{3}CBP and sulfur radical cations in H_2O and D_2O in our steady-state photolysis systems were quantified by a chemical dosimeter based on reaction 15 between ^{3}CBP and DMS in N_2-saturated aqueous (H_2O or D_2O) solutions, pH 7.0, containing 2.5×10^{-4} M CBP and various concentrations of DMS between 2×10^{-3} M and 3.4×10^{-2} M.

The quenching of ^{3}CBP by DMS in aqueous solution occurs with $k_9 = 1.5 \times 10^9$ M^{-1} s^{-1}.[9] By laser-photolysis the respective quantum yields Φ for processes 10−15 in H_2O and D_2O were determined at both pL 6.7 and pL 10 (L = H, D).[10] These quantum yields are essentially independent of pL in this region. A non-productive reaction of ^{3}CBP with DMS to yield ground-state CBP occurs with $\Phi_{n,H_2O} = 0.72$ and $\Phi_{n,D_2O} = 0.77$. These nonproductive pathways represent either physical quenching (reaction 10) or back-electron transfer (reaction 12) within the initially formed charge-transfer complex **6** (reaction 11). Competitively, complex **6** decomposes via electron transfer (reactions 13 and 14) ($\Phi_{el,H_2O} = 0.17$ and $\Phi_{el,D_2O} = 0.10$, related to initial [^{3}CBP]), and hydrogen transfer (reaction 15) ($\Phi_{H,H_2O} = 0.12$ and $\Phi_{H,D_2O} = 0.13$). Thus, only the electron transfer pathway shows a significant normal product isotope effect of $\Phi_{el,H_2O}/\Phi_{el,D_2O} = 1.7$. This mechanism initially yields $\mathbf{7}^-$ which will protonate, depending on pH ($pK_{a,16} = 8.2$[11]). Depending on the actual concentration of DMS, the monomeric **1a** will associate with DMS to yield the dimeric species **2a** (reaction 17; $K_{17} = 2.0 \times 10^5$ M^{-1}).[12]

$$^3\text{CBP} + CH_3SCH_3 \rightarrow \text{products} \tag{9}$$

$$^3\text{CBP} + CH_3SCH_3 \rightarrow \text{CBP} + CH_3SCH_3 \tag{10}$$

$$^3\text{CBP} + CH_3SCH_3 \rightleftharpoons [^{\delta-}\text{CBP}\cdots S<^{\delta+}] \ (\mathbf{6}) \tag{11}$$

$$\mathbf{6} \rightarrow \text{CBP} + CH_3SCH_3 \tag{12}$$

$$\mathbf{6} + H^+ \rightarrow (PhCO_2^-)(Ph)C^{\bullet}\text{-OH} \ (\mathbf{7}) + (CH_3)_2S^{\bullet +} \ (\mathbf{1a}) \tag{13}$$

$$\mathbf{6} \rightarrow (PhCO_2^-)(Ph)C^{\bullet}\text{-}O^- \ (\mathbf{7}^-) + \mathbf{1a} \tag{14}$$

$$\mathbf{6} \rightarrow \mathbf{7} + {}^{\bullet}CH_2SCH_3 \tag{15}$$

$$\mathbf{7}^- + H^+ \rightleftharpoons \mathbf{7} \tag{16}$$

$$\mathbf{1a} + >S \underset{k_{-17}}{\overset{k_{17}}{\rightleftharpoons}} [(CH_3)_2S\therefore S(CH_3)_2]^+ \ (\mathbf{2a}) \tag{17}$$

By measurement of the photolytic yield of reaction 15 in our steady-state system we will be able to obtain the photolytic yields of the electron transfer pathways (reactions 13 and 14) based on the ratio of Φ_{el}/Φ_H established by laser photolysis[10] for the ^{3}CBP/DMS system.

At neutral pH, there are two possible pathways to irreversibly consume CBP in the absence of oxygen, namely reactions 18 (formation of pinacol **8**) and 19. On the other hand, reverse electron transfer from **7** (or $\mathbf{7}^-$) to **1a** or **2a**, respectively, will reconstitute ground state CBP (reaction 20).

$$2\mathbf{7} \rightarrow (PhCO_2^-)(Ph)(HO)C\text{-}C(OH)(Ph)(PhCO_2^-) \ (\mathbf{8}) \tag{18}$$

$$\mathbf{7} + {}^{\bullet}CH_2SCH_3 \rightarrow (PhCO_2^-)(Ph)(HO)C\text{-}CH_2SCH_3 \ (\mathbf{9}) \tag{19}$$

$$\mathbf{7} + \mathbf{1a}/\mathbf{2a} \rightarrow H^+ + \text{DMS}/2\text{DMS} + \text{CBP} \tag{20}$$

In order to obtain a quantitative relationship between the consumption of CBP and the initial yield of ^{3}CBP we have to ensure that any deprotonation of **1a** (reaction 21) will not compete against the reverse electron transfer reaction 20.

$$\mathbf{1a} \rightarrow {}^{\bullet}CH_2SCH_3 + H^+ \tag{21}$$

This deprotonation reaction proceeds significantly faster from the monomeric species **1a** than from the dimer **2a**. Given that the irreversible deprotonation from **1a** could remove **1a**/**2a** from the solution, then the consumption of CBP should be dependent on the concentration of DMS. With increasing DMS concentrations the final consumption of CBP should become representative for reactions 15, 18 and 19 since high DMS concentrations stabilize **2a**, available for reverse electron transfer. In fact, during pulse radiolysis experiments at DMS concentrations $>10^{-2}$ M, species **2a** was observed to entirely decay via second-order radical−radical reactions, indicating that deprotonation via reactions −17 and 21 is negligible at such high DMS concentrations.[13,14]

(4) Merényi, G.; Lind, J.; Engman, L. *J. Phys. Chem.* **1996**, *100*, 8875−8881.
(5) (a) Bobrowski, K.; Schöneich, Ch. *J. Chem. Soc., Chem. Commun.* **1993**, 795−797. (b) Schöneich, Ch.; Bobrowski, K. *J. Phys. Chem.* **1994**, *98*, 12613−12620.
(6) Eriksen, J.; Foote, C. S.; Parker, T. L. *J. Am. Chem. Soc.* **1977**, *99*, 6455−6456.
(7) Ando, W.; Kabe, Y.; Kobayashi, S.; Takyu, C.; Yamagishi, A.; Inaba, H. *J. Am. Chem. Soc.* **1980**, *102*, 4526−4528.
(8) Inoue, K.; Matsuura, T.; Saito, I. *Tetrahedron* **1985**, *41*, 2177−2181.
(9) Bobrowski, K.; Marciniak, B.; Hug, G. L. *J. Photochem. Photobiol., A* **1994**, *81*, 159−168.
(10) Bobrowski, K.; Hug, G. L.; Marciniak, B.; Miller, B. L.; Schöneich, Ch., manuscript in preparation
(11) Inbar, S.; Linschitz, H.; Cohen, S. G. *J. Am. Chem. Soc.* **1981**, *103*, 7323−7328.
(12) Mönig, J.; Goslich, R.; Asmus, K.-D. *Ber. Bunsenges. Phys. Chem.* **1986**, *90*, 115−121.
(13) Bonifačić, M.; Möckel, H.; Bahnemann, D.; Asmus, K.-D. *J. Chem. Soc. Perkin Trans. 2* **1975**, 675−685.

Table 1. Rate Constants Used or Determined in this Paper

process	rate constant	ref
k_3	2.6×10^9 M^{-1} s^{-1}	35
k_6	1.1×10^8 M^{-1} s^{-1}	4,5
k_8	$(2.3 \pm 1.2) \times 10^{11}$ M^{-1} s^{-1}	this work
k_9	1.5×10^9 M^{-1} s^{-1}	9
k_{22}	4.2×10^6 M^{-1} s^{-1}	11
k_{23}	1.5×10^5 s^{-1}	11
k_{26}	$(3.5 \pm 0.3) \times 10^7$ M^{-1} s^{-1}	this work
k_{27}	$\leq 3.0 \times 10^4$ M^{-1} s^{-1}	this work
k_{28}	4.0×10^9 M^{-1} s^{-1}	20
k_{31}	$\leq 5.0 \times 10^9$ M^{-1} s^{-1}	estimated from 23
k_{33}	$\leq 1.0 \times 10^8$ M^{-1} s^{-1}	estimated from 28
k_{37}	$\approx 10^2$ M^{-1} s^{-1}	estimated from 26
k_{56}	2.0×10^9 M^{-1} s^{-1}	34

The photolysis of our N_2-saturated aqueous solutions yields a final consumption of CBP of $(5.0 \pm 0.5) \times 10^{-7}$ M s^{-1} regardless of DMS concentrations between 2×10^{-3} M and 3.4×10^{-2} M, and regardless of whether the reaction was performed in H_2O or D_2O (because of the broader spectrum of incident light in the steady-state photolysis experiments the yields are presented in units of M s^{-1} rather than quantum yields in order to avoid confusion with laser photolysis experiments employing a defined wavelength of incident light; see Experimental). For a quantitative assessment we have to take into account that ^{3}CBP can competitively suffer physical quenching according to reactions 22 ($k_{22} = 4.2 \times 10^6$ M^{-1} s^{-1}) and 23 ($k_{23} = 1.5 \times 10^5$ s^{-1}).[11]

$$^3\text{CBP} + \text{CBP} \rightarrow 2\text{CBP} \quad (22)$$

$$^3\text{CBP} \rightarrow \text{CBP} \quad (23)$$

Table 1 summarizes all rate constants used or determined in this paper. With $k_9 = 1.5 \times 10^9$ M^{-1} s^{-1}, we derive that at [DMS] $\geq 2.0 \times 10^{-3}$ M more than 95% of ^{3}CBP will directly attack DMS. Thus, the yield of CBP consumption at [DMS] $\geq 2.0 \times 10^{-3}$ M should be representative for reactions 15, 18, and 19. On the basis that reaction 15 leads to the consumption of 1 equiv CBP per hydrogen transfer event, and the quantum yields[10] $\Phi_{H,H_2O} = 0.12$ and $\Phi_{H,D_2O} = 0.13$, we calculate that the initial yield of ^{3}CBP in our steady-state system is on the order of $(4.2 \pm 0.5) \times 10^{-6}$ M s^{-1} in both solvents H_2O and D_2O, respectively.

From the ratios[10] $[\Phi_{el}/\Phi_H]_{H_2O} = 1.42$ and $[\Phi_{el}/\Phi_H]_{D_2O} = 0.77$ we derive that the electron transfer processes (reactions 13 and 14) should generate **1a**/**2a** at levels of $\Phi_{el,H_2O} \times [^3\text{CBP}] = 7.1 \times 10^{-7}$ M s^{-1} in H_2O and $\Phi_{el,D_2O} \times [^3\text{CBP}] = 3.85 \times 10^{-7}$ M s^{-1} in D_2O. As we will see in the discussion, these yields are well in accord with the observed material balances.

B. The Aerobic Oxidation of DMS to Dimethyl Sulfoxide by ^{3}CBP. 1. Influence of pH, Superoxide Dismutase, and Oxygen Concentration. Figure 1A,B display the yields of dimethyl sulfoxide (DMSO) obtained as a function of pH during the photolysis of air-saturated aqueous (H_2O) solutions, containing 2.5×10^{-4} M CBP, 1.0×10^{-2} M sodium phosphate, and 6.8×10^{-3} M DMS (system I) or 3.4×10^{-2} M DMS (system II), respectively. At pH values between 6.2 and 10, the total DMSO yields are rather constant and drop only slightly at pH 11 (curves a). A significant reduction of the DMSO yields (e.g. by 90% at pH 6.2 for 3.4×10^{-2} M DMS) is observed when the experiments are performed in the presence of 1000 U/mL Cu,Zn superoxide dismutase (SOD) (curves c), corresponding to 6.7×10^{-6} M SOD dimer (taking a specific activity of 4400 U/mg and a molecular weight of 34 000 Da for the SOD dimer). These remaining yields will be referred to as *SOD-independent* yields. Identical results as with 1000 U/mL SOD were obtained with 500 U/mL and 2000 U/mL SOD, respectively (data not shown), indicating that the SOD effect was independent of the SOD concentration at these SOD levels, and therefore at maximum. A tendency of increasing *SOD-independent* DMSO yields is observed with increasing pH in the presence of 1000 U/mL Cu,Zn superoxide dismutase (SOD) (curves c). Subtraction of the *SOD-independent* yields from the total DMSO yields gives the *SOD-dependent* DMSO yields (curves b). The latter show rather constant values between pH 6.2 and 9.0 and drop significantly only for pH > 9.0 at high concentrations of DMS (curves b). By assessing the SOD activity before and after each experiment we confirmed that there was no measurable inactivation of the enzyme during the photolysis.

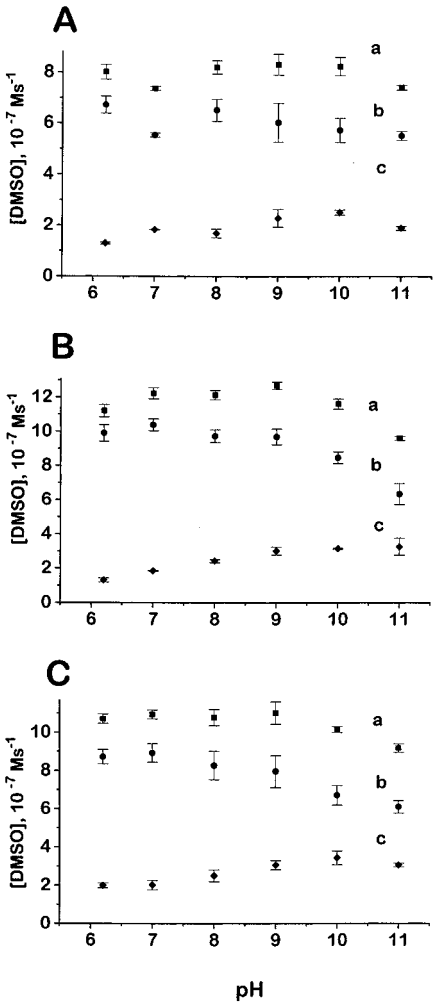

Figure 1. Photolytic yields of DMSO as a function of pH. Air-saturated aqueous solutions, containing 2.5×10^{-4} M CBP, 1.0×10^{-2} M phosphate buffer, and (A) 6.8×10^{-3} M DMS (system I) or (B) 3.4×10^{-2} M DMS (system II). (C) Oxygen-saturated solution containing 2.5×10^{-4} M CBP, 1.0×10^{-2} M phosphate buffer, and 3.4×10^{-2} M DMS (system III). Curves a (■): total DMSO yields in absence of SOD; curves b (●): SOD-dependent DMSO yields obtained by subtraction of curves c from curves a; curves c (◆): SOD-independent DMSO yields obtained in the presence of 1,000 U/mL SOD.

Figure 1C displays the DMSO yields obtained after photolysis of oxygen-saturated aqueous (H_2O) solutions containing 1.0×10^{-2} M sodium phosphate, 2.5×10^{-4} M CBP, and 3.4×10^{-2} M DMS (system III) at various pH. It is important to note that there is no significant difference between the total DMSO yields obtained with 3.4×10^{-2} M DMS under conditions of air−saturation and oxygen−saturation, respectively (curves a in

(14) Asmus, K.-D. In *Sulfur-Centered Reactive Intermediates in Chemistry and Biology*; Chatgilialoglu, C., Asmus, K.-D., Eds; NATO ASI Series: Plenum Press: New York, 1990; Vol. 197, 155−172.

Table 2. Yields of DMSO as a Function of DMS Concentration and SOD[a]

	DMSO, 10^{-7} M s^{-1}		
SOD, U/mL	0.68×10^{-2} M DMS	2.04×10^{-2} M DMS	3.4×10^{-2} M DMS
0	8.20 ± 0.2	9.61 ± 0.41	11.7 ± 0.7
500	1.71 ± 0.13	2.59 ± 0.03	3.48 ± 0.05
1000	1.78 ± 0.02	2.27 ± 0.06	3.67 ± 0.17

[a] Air-saturated solutions, pH 8.0, containing 2.5×10^{-4} M CBP and 1.0×10^{-2} M sodium phosphate.

Figure 1B,C). However, in particular at pH 6−7 there is a larger fraction of *SOD-independent* DMSO formation (curve c) in the oxygen-saturated system.

In contrast to oxygen-containing solutions there was no significant sulfoxide formation during the photolysis of N_2-saturated solutions. This result demonstrates the importance of oxygen in the mechanistic scheme. Under our experimental conditions this can be rationalized by the competition of reverse electron transfer (reaction 20) with disproportionation. However, in earlier radiation chemical experiments we had excluded that disproportionation of **1a** or **2a** contributes to sulfoxide formation even under conditions where reverse electron transfer reactions are absent, i.e., in the absence of species such as **7** and $\mathbf{7}^-$.[3]

Table 2 displays the *SOD-independent* DMSO yields obtained as a function of DMS concentration at pH 8.0 (air-saturated aqueous solution containing 2.5×10^{-4} M CBP and 1.0×10^{-2} M sodium phosphate). An important feature is that the yields of DMSO gradually increase with increasing DMS concentration independent of the absence or presence of 500 or 1000 U/mL SOD.

2. Native SOD and Demetalated Apoenzyme. Sulfide radical cations such as **1a** or **2a** are very strong one-electron oxidants.[15] Therefore, we had to design an experiment to confirm that the inhibition of sulfoxide formation by SOD was not merely caused by the competitive reaction of sulfide radical cations with easily oxidizable amino acids X of the SOD protein skeleton (reaction 24) where X in bovine erythrocyte SOD could be Tyr or Met.[16,17]

$$\mathbf{2a} + \text{SOD-(X)} \rightarrow 2{>}\text{S} + \text{SOD-(X}^{\bullet+}\text{)} \qquad (24)$$

For this purpose a demetalated des-Cu variant (apo-SOD) of SOD was prepared by partial unfolding of the enzyme, extraction of Cu^{2+} with EDTA, and refolding (see *Experimental*). Figure 2A displays the activities of native enzyme and apoenzyme in terms of inhibition of the reduction of ferricytochrome c by superoxide, generated by the xanthine/xanthine oxidase system. The apo-SOD shows approximately 9% of the activity as compared to the native enzyme, essentially comparable to the preparation of apoenzyme by McCord and Fridovich.[18] This residual activity is most probably caused by an incomplete removal of Cu^{2+}. When air-saturated solutions containing 1.0×10^{-2} M sodium phosphate, pH 8.0, 2.5×10^{-4} M CBP, and 3.4×10^{-2} M DMS were photolyzed in the presence of either native SOD or apoenzyme, the apoenzyme was much less effective in inhibiting the formation of DMSO than was native SOD, as shown in Figure 2B. These data suggest that it is the dismutation of superoxide by SOD which causes the observed

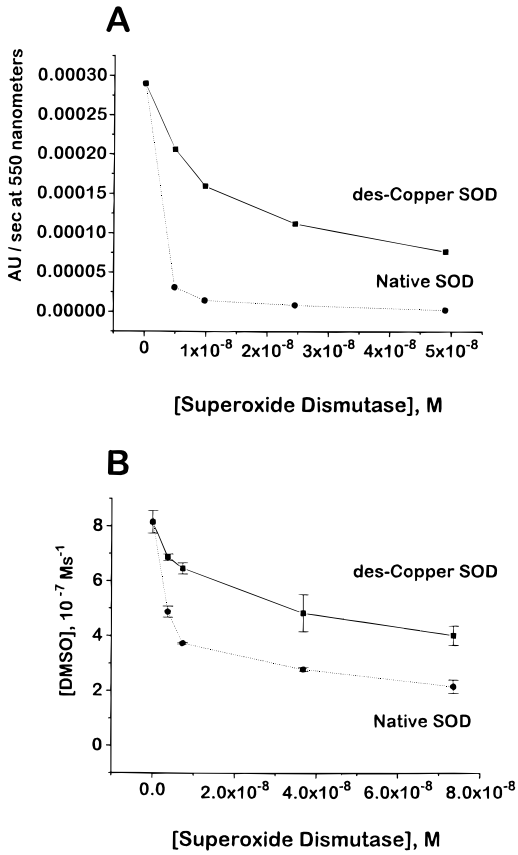

Figure 2. (A) Activity of native and des-Cu SOD at inhibiting the xanthine/xanthine oxidase induced reduction of cytochrome c. (B) Efficiency of various concentrations of native and des-Cu SOD at inhibiting the photolytic formation of DMSO; conditions: air-saturated aqueous solutions, pH 8.0, containing 2.5×10^{-4} M CBP, 3.4×10^{-2} M DMS, and 1.0×10^{-2} M phosphate buffer.

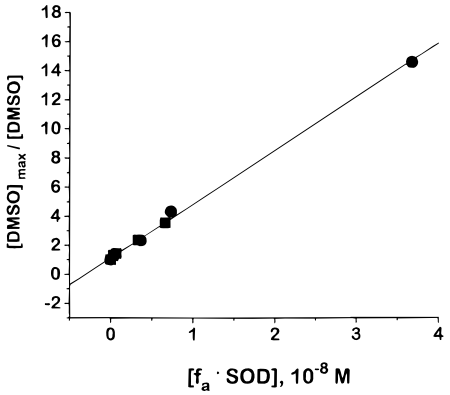

Figure 3. Competition plot displaying the effect of the active fraction of SOD on the photolytic formation of DMSO (conditions as for Figure 2B). The active fractions of SOD were obtained by multiplication of the enzyme concentration with $f_a = 1.0$ for native and $f_a = 0.09$ for des-Cu SOD. Native SOD: ●, des-Cu SOD: ■. Data were corrected for SOD-*independent* DMSO through processes not initiated by sulfur radical cation formation, i.e., from the measured DMSO yields at various (low) SOD concentrations between 5×10^{-10} and 3.7×10^{-8} M were subtracted the DMSO yields at high SOD concentrations of 6.7×10^{-6} M.

inhibition of sulfoxide formation and not an unspecific oxidation of amino acid residues of SOD by **2a** according to reaction 24.

The fact that the apoenzyme still inhibits sulfoxide formation, though to lesser extent, can be related to its residual 9% SOD activity. This becomes evident from Figure 3 which shows a plot of $[DMSO]_{max}/[DMSO]$ vs $f_a[SOD]$ where $[DMSO]_{max}$ and [DMSO] represent the yields of DMSO in the absence and presence of SOD, respectively, f_a represents the fraction of active

(15) Bonifačić, M.; Weiss, J.; Chaudhri, S. A.; Asmus, K.-D. *J. Phys. Chem.* **1985**, *89*, 3910−3914.
(16) Keele, Jr., B. B.; McCord, J. M.; Fridovich, I. *J. Biol. Chem.* **1971**, *246*, 2875−2880.
(17) Forman, H. J.; Evans, H. J.; Hill, R. L.; Fridovich, I. *Biochemistry* **1973**, *12*, 823−827.
(18) McCord, J. M.; Fridovich, I. *J. Biol. Chem.* **1969**, *244*, 6049−6055.

SOD, and [SOD] represents the concentration of SOD dimer. In this plot all the points fall on a line regardless whether obtained with native SOD or apoenzyme.

3. Exclusion of a Direct Oxidation of DMS to DMSO by Superoxide. The fact that SOD inhibits the formation of DMSO necessitates experimental evidence as to what role superoxide plays during the oxidation reaction. One potential pathway would be the direct oxidation of DMS to DMSO by superoxide or its conjugate acid, HOO• (reaction 25).

$$(CH_3)_2S + O_2^{\bullet -} \rightarrow (CH_3)_2S{=}O + \text{products} \qquad (25)$$

A series of experiments was carried out in oxygen-saturated aqueous (D_2O) solution, pD 10, containing 1.0×10^{-2} M sodium phosphate, 2.5×10^{-4} M CBP, 6.8×10^{-3} M DMS, and (i) no further additive, (ii) 1.33 M sodium formate, or (iii) 1.33 M sodium acetate. Conditions of pD 10 were selected in order to accelerate superoxide formation from **7** (via $\mathbf{7}^-$; see below) and to slow down the bimolecular dismutation of superoxide.[19] Analysis of the photolyzed reaction mixtures by ^{1}H-NMR revealed that identical yields of DMSO were formed in the absence of any further additive and in the presence of 1.33 M sodium acetate, respectively, whereas the presence of 1.33 M sodium formate caused a 65% reduction of the DMSO yields (^{1}H-NMR analysis was preferred to HPLC for these experiments since the high salt concentrations compromised the retention behavior of DMS, DMSO, and CBP during reversed phase chromatography).

$$^3\text{CBP} + HCO_2^- \rightarrow \mathbf{7} + {}^\bullet CO_2^- \qquad (26)$$

$$^3\text{CBP} + CH_3CO_2^- \rightarrow \mathbf{7} + {}^\bullet CH_2CO_2^- \qquad (27)$$

$${}^\bullet CO_2^- + O_2 \rightarrow CO_2 + O_2^{\bullet -} \qquad (28)$$

$${}^\bullet CO_2^- + \text{CBP} \rightarrow CO_2 + \mathbf{7}^- \qquad (29)$$

$$\mathbf{7}^- + O_2 \rightarrow \text{CBP} + O_2^{\bullet -} \qquad (30)$$

From competition experiments (see below) we obtained $k_{26} = (3.5 \pm 0.3) \times 10^7$ M^{-1} s^{-1} and $k_{27} \leq 3 \times 10^4$ M^{-1} s^{-1}. In the acetate-containing system, superoxide should be formed via a sequence of reactions 13−16 and 30, and the extent of reaction 27 should be negligible (k_9[DMS] $\gg k_{27}$[$CH_3CO_2^-$]). Reaction 30 will be rapid at pD 10. Thus, we expect 1 equiv of $O_2^{\bullet -}$ per equivalent of ^{3}CBP in the acetate-containing system. The ${}^\bullet CO_2^-$ radical anion rapidly reduces molecular oxygen either directly (reaction 28; $k_{28} = 4 \times 10^9$ M^{-1} s^{-1} [20]) or via initial reduction of ground state CBP (analogous to the reaction between $(CH_3)_2C^\bullet$-OH and CBP) followed by reaction 30. Thus, the reaction sequence 26 and 28−30 yields 2 equiv of superoxide per equivalent of ^{3}CBP reacting with formate. Competition kinetics predict that, in the presence of 1.33 M sodium formate and 6.8×10^{-3} M DMS, a fraction of 82% of ^{3}CBP should directly react with formate, overall producing a 1.8 fold higher yield of $O_2^{\bullet -}$ in the formate system than in the acetate system. However, in the formate system we observe a 65% reduction of the formation of DMSO which (i) suggest that superoxide does not directly oxidize DMS under our experimental conditions, and (ii) is reasonably close to the expected drop of the DMSO yields (82%) based on competition kinetics (any significant direct oxidation of either DMS or **2a** by the dismutation product H_2O_2 can also be excluded since then we would not expect any protection by SOD which dismutates superoxide to H_2O_2).

(19) Bielski, B. H. J.; Cabelli, D. E. *Int. J. Radiat. Biol.* **1991**, *59*, 291−319.

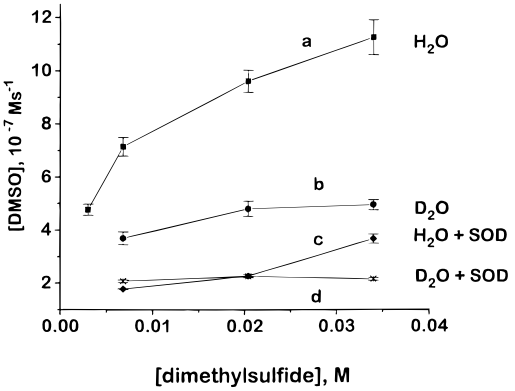

Figure 4. Solvent isotope effect on the photolytic formation of DMSO. Conditions: Aqueous (L_2O, L = H, D) solutions, pL 8.0, containing 1.0×10^{-2} M phosphate buffer, 2.5×10^{-4} M CBP, various concentrations DMS, and no (curves a and b) or 1,000 U/mL superoxide dismutase (curves c and d).

4. The Rate Constants k_{26} and k_{27}. The rate constant k_{26} was determined by standard competition kinetics measuring the decomposition of CBP, −d[CBP], in N_2-saturated aqueous solutions, pH 7.0, containing 2×10^{-2} M sodium phosphate, 2.5×10^{-4} M CBP, and various concentrations of sodium formate.

A plot of d[-CBP]$_{max}$/[-CBP] vs formate concentration yielded a straight line with a slope equal to ($k_{22} + k_{23}$ [CBP])/k_{26} from which $k_{26} = (3.5 \pm 0.3) \times 10^7$ M^{-1} s^{-1} was derived. There was no measurable decomposition of CBP in the presence of up to 5.0×10^{-2} M sodium acetate instead of formate, and we can obtain an upper limit of [-CBP]$_{max}$/[CBP] $\geq$ 100 for [acetate] $\leq 5.0 \times 10^{-2}$ M which leads to $k_{27} \leq 3.0 \times 10^4$ M^{-1} s^{-1}.

5. Solvent Isotope Effects. Figure 4 displays the yields of DMSO obtained as a function of L_2O (L = H, D) for the photolysis of various concentrations of DMS in air-saturated aqueous solutions containing 1.0×10^{-2} M sodium phosphate, pL = 8.0, and 2.5×10^{-4} M CBP. There are several important features. (i) The total yields of DMSO are significantly higher in H_2O (curve a) as compared to D_2O (curve b), i.e., by a factor of 1.94 for [DMS] = 6.8×10^{-3} M and 2.04 at [DMS] = 3.4×10^{-2} M. (ii) The *SOD-independent* pathway in the presence of 1,000 U/mL SOD (curves c and d) produced DMSO to comparable extents in H_2O and D_2O for [DMS] $\leq 2.0 \times 10^{-2}$ M. However, for 3.4×10^{-2} M DMS the *SOD-independent* pathway gave 1.58 times higher yields of DMSO in H_2O (3.67×10^{-7} M s^{-1}) than in D_2O (2.32×10^{-7} M s^{-1}). There were no differences between experiments employing 500, 1000, or 2000 U/mL SOD in both H_2O and D_2O, indicating that an SOD activity of 1,000 U/mL was sufficient for suppressing the *SOD-dependent* pathway in both solvents. These results mean that in D_2O a larger fraction of DMSO is generated via the *SOD-independent* pathway though the total yields of sulfoxide are significantly smaller than in H_2O. This is particularly obvious for the smaller DMS concentrations. The variation of oxygen concentration between 2.5×10^{-4} M (air-saturated) and 1.25×10^{-3} M (oxygen-saturated) had little influence on the total DMSO formation in H_2O, as displayed in Figure 5. Only in D_2O an effect is noticable for 6.8×10^{-3} M DMS where the yield of DMSO increases from 3.7×10^{-7} M s^{-1} in air-saturated solution to 4.7×10^{-7} M s^{-1} in oxygen-saturated solution.

6. The Source of Oxygen: Experiments with $^{16}O_2$ in $^{18}OH_2$. The source of the oxygen in DMSO was determined by GC-MS experiments subsequent to the photolysis of air-saturated ($^{16}O_2/N_2$, 1:4, v/v) solutions containing 1.25×10^{-4}

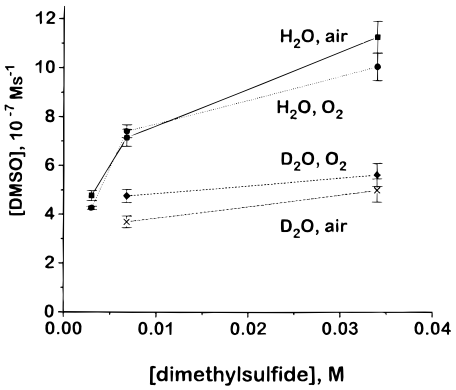

Figure 5. Influence of oxygen concentration of the photolytic formation of DMSO in H_2O and D_2O at various concentrations of DMS. Conditions: Aqueous solutions (L_2O, L = H, D), pL = 8.0, containing 2.5×10^{-4} M CBP and 1.0×10^{-2} M phosphate buffer.

M CBP and 2.0×10^{-2} M sodium phosphate, pL 10 (L = H or D), in either $H_2{}^{18}O$, $H_2{}^{18}O/H_2{}^{16}O$ (1:1, v/v), or $H_2{}^{18}O/D_2{}^{16}O$ (1:1, v/v), respectively. The results are summarized in Table 3. In control experiments we analyzed synthetic $DMS^{16}O$ dissolved in $H_2{}^{18}O$ (entry 2), and $DMS^{18}O$ in $H_2{}^{16}O$ (entry 3). There was no oxygen exchange between DMSO and water under our experimental conditions. Further control experiments (entries 9−11) were done particularly with regard to the possible incorporation of deuterium into DMSO during photolytic reactions carried out in $D_2O/H_2{}^{18}O$ mixtures (entry 7). There was no incorporation of deuterium into DMSO during photolytic oxidation of DMS in D_2O (entries 10 and 11), showing that the significant yield of the isotopic cluster of $m/z = 80$ in entry 7 is caused by the incorporation of ^{18}O from the solvent.

In general, the incorporation of ^{18}O into DMSO is small under all experimental conditions, indicating that the oxygen is derived mainly from molecular oxygen ($^{16}O_2$). However, we find that a significantly higher fraction of $DMS^{18}O$ is present whenever the experiments are carried out in the presence of SOD. Even higher levels of ^{18}O incorporation into DMSO are detectable when the experiments are carried out in mixtures of H_2O and D_2O. Mechanistically we can conclude that sulfoxide formation via the SOD-*independent* pathway involves at least one intermediate different from the intermediate formed in the absence of SOD (hence different fractions of ^{18}O incorporation under both experimental conditions). Furthermore, the incorporation of ^{18}O is promoted by the presence of D_2O.

7. The Formation of Formaldehyde. There is little variation of formaldehyde yields over a range of pH 6.2−11.0, representatively measured for system II, with an average formation of $(7.3 \pm 0.6) \times 10^{-7}$ M s^{-1}. The additional presence of 1000 U/mL SOD had no influence on the formaldehyde yields.

8. Other Reaction Products. In order to obtain a complete material balance we monitored the formation of several other possible reaction products which could originate from the oxidation and subsequent reactions of DMS. The yields of methanethiol (CH_3SH), dimethyldisulfide (CH_3SSCH_3), methanesulfonic acid (CH_3SO_3H), and dimethylsulfone ($(CH_3)_2SO_2$) were quantified by ^{1}H-NMR by comparison to known quantities of authentic standards, as displayed in Table 4.

It is evident that all the products listed in Table 4 are formed with only minor yields when compared to the yields of dimethyl sulfoxide and formaldehyde.

C. The Aerobic Oxidation of Diethyl Sulfide by ^{3}CBP. Conclusive information with regard to the involvement of dimeric sulfur radical cations in the sulfoxide formation can be obtained from a comparison of the sulfoxide yields from the photolysis of DMS and diethyl sulfide (DES), respectively. Table 5 compares the yields of diethylsulfoxide (DESO) and DMSO obtained after photolysis of air-saturated aqueous solutions containing 2.5×10^{-4} M CBP and 1.0×10^{-2} M sodium phosphate, pH 7.0, in the absence and the presence of SOD.

The most notable feature is that the ratio of total sulfoxide yields to the *SOD-independent* sulfoxide yields are much lower for DES than for DMS, in particular at the lower sulfide concentration. The *SOD-independent* DESO yields are higher than the *SOD-independent* DMSO yields at both sulfide concentrations.

Discussion

1. Sulfur Radical Cations as Intermediates for Sulfoxide Formation in the *SOD-Dependent* But Not the *SOD-Independent* Pathway. During the photooxidation of DMS by ^{3}CBP in oxygen-containing solutions, sulfur radical cations can theoretically form via two distinct pathways. A type I mechanism is based on the direct one-electron oxidation of DMS by ^{3}CBP (reactions 11, 13, 14, and 17). Alternatively, the interaction of ^{3}CBP with triplet molecular oxygen can generate singlet oxygen (reaction 31).[21−23]

$$^3\text{CBP} + {}^3\text{O}_2 \rightarrow \text{CBP} + {}^1\text{O}_2(^1\Delta_g, {}^1\Sigma^+_g) \qquad (31)$$

Singlet oxygen could theoretically produce sulfur radical cations via one-electron oxidation of DMS (reaction 32) although this process appears rather unlikely in light of the fact that such electron transfer mechanisms gave small yields only with electron rich sulfides.[8]

$$^1\text{O}_2 + {>}\text{S} \rightarrow \mathbf{1a} + \text{O}_2^{\bullet -} \qquad (32)$$

Singlet oxygen rather adds to DMS to produce the zwitterionic intermediate **10** (reaction 33).[1]

$$^1\text{O}_2 + {>}\text{S} \rightleftharpoons {>}\text{S}^{(+)}\text{-O-O}^{(-)}\ (\mathbf{10}) \qquad (33)$$

We note that in water the lifetime of **10** may be rather short not only because of its reaction with a second DMS to yield 2 equiv of DMSO per equivalent of **10** (reaction 34)[1] but also due to a possible addition of HO^-/H^+ to yield a hydroperoxy sulfurane, HO-S$(CH_3)_2$-OOH (**11**) (see below).

$$\mathbf{10} + {>}\text{S} \rightarrow 2{>}\text{S}{=}\text{O} \qquad (34)$$

For our mechanistic considerations of the *SOD-dependent* pathway of sulfoxide formation the mere formation of sulfur radical cations **1a**, regardless whether via reactions 11, 13, and 14 or reaction 32, would be sufficient. However, for a quantitative assessment of sulfoxide formation via the *SOD-independent* pathway, it is important to determine the potential relative contributions of singlet oxygen (via the initial intermediate **10**; reactions 33 and 34) and the *hydroxide pathway* (reactions 3−7).

The individual processes of reaction 31 are currently under extensive investigation with regard to the yields of singlet oxygen and intermediates such as exciplexes.[21−23] In general, it appears that the efficiency of singlet oxygen formation, S_Δ, decreases with decreasing oxidation potential of the sensitizer and increasing rate constant of the quenching process.[23] By comparison with values for benzophenone in solvents of

(20) Simic, M. G. *Methods Enzymol.* **1990**, *186*, 89−100.
(21) McLean, A. J.; Rodgers, M. A. J. *J. Am. Chem. Soc.* **1992**, *114*, 3145−3147.
(22) McLean, A. J.; Rodgers, M. A. J. *J. Am. Chem. Soc.* **1993**, *115*, 9874−9875.
(23) Grewer, C.; Brauer, H.-D. *J. Phys. Chem.* **1994**, *98*, 4230−4235.

Table 3. Incorporation of ^{18}O into DMSO in the Absence and Presence of SOD and D_2O[a]

	system	±SOD	DMSO molecular ion (MW 78) isotopic cluster *m/z* 80 as % *m/z* 80[a]	incorporation of ^{18}O (%)[c]
1	$DMS^{16}O/H_2{}^{16}O$		4.60 ± 0.37	
2	$DMS^{16}O/H_2{}^{18}O$		4.60 ± 0.40	0.0
3	$DMS^{18}O/H_2{}^{16}O$		94.0	94.0
4	$DMS^{16}O/H_2{}^{16}O$ control, entries 5−7		4.51 ± 0.04	
5	3.4×10^{-2} M DMS,	−SOD	7.14 ± 0.01[b]	2.63
hν	$H_2{}^{18}O$, pH 10	+SOD	10.4 ± 0.28[b]	5.90
6	3.4×10^{-2} M DMS,			
hν	$H_2{}^{18}O/H_2{}^{16}O$ (1:1),	−SOD	5.03 ± 0.5[b]	0.52
	pH 10	+SOD	5.94 ± 0.4[b]	1.43
7	3.4×10^{-2} M DMS,			
hν	$H_2{}^{18}O/D_2{}^{16}O$ (1:1),	−SOD	7.61 ± 0.26[b]	3.10
	pH 10	+SOD	8.09 ± 0.12[b]	3.58
8	$DMSO/H_2{}^{16}O$ control, entries 9−11		4.63 ± 0.06	
9	3.0×10^{-2} M DMSO/ $D_2{}^{16}O$, pD 10, no h*ν*	+SOD	4.75 ± 0.09	(0.12)[d]
10	3.0×10^{-2} M DMS/	+SOD	4.50 ± 0.42	0
hν	$D_2{}^{16}O$, pD10, +catalase			
11	3.0×10^{-2} M DMS,	+SOD	4.66 ± 0.09	0
hν	$D_2{}^{16}O$, pD 10			

[a] Standard deviation from $n = 3$. [b] $n = 2$. [c] *m/z* 80 from isotopic experiment corrected for experimental control value for natural abundance. The predicted natural abundance of the DMSO molecular ion isotopomers is *m/z* 78 (100%) and *m/z* 80 (4.67%). [d] Incorporation of trace amount of deuterium. [e] Photolytic experiments (entries 5−7, 10, and 11, labeled *hν*), are air-saturated and contain 1.25×10^{-4} M CBP.

Table 4. Reaction Products from the Photolytic Oxidation of 1.0×10^{-2} M DMS in N_2- and O_2-Saturated Solution Exposed to a Photon Flux of 1.48×10^{-5} M photons/s at 350 nm

		yield, M s^{-1}			
conditions	pH	CH_3SH	CH_3SSCH_3	CH_3SO_3H	$CH_3SO_2CH_3$
N_2-sat	6.5			1.23×10^{-8}	
N_2-sat	12.0	6.5×10^{-8}	1.23×10^{-8}	5.5×10^{-9}	
O_2-sat	6.5	5.0×10^{-8}	1.4×10^{-7}	6.6×10^{-8}	2.4×10^{-8}
O_2-sat	12.0			2.72×10^{-8}	

Table 5. Photolytic Yields of Sulfoxide in Air-Saturated Solutions, pH 7, Containing 2.5×10^{-4} M CBP, 1.0×10^{-2} M Sodium Phosphate, and Various Concentrations of Sulfide and SOD

sulfide	concentration	±1000 U/mL SOD	sulfoxide, 10^{-7} M s^{-1}	ratio[a]
DMS	0.68×10^{-2} M	−SOD	7.4 ± 0.2	4.1
		+SOD	1.8 ± 0.1	
DES	0.68×10^{-2} M	−SOD	4.6 ± 0.3	1.3
		+SOD	3.5 ± 0.1	
DMS	3.4×10^{-2} M	−SOD	12.2 ± 0.3	6.8
		+SOD	1.8 ± 0.1	
DES	3.4×10^{-2} M	−SOD	8.4 ± 0.5	1.7
		+SOD	5.0 ± 0.3	

[a] [Total sulfoxide]/[sulfoxide in presence of SOD].

different polarity[23] we estimate that for CBP in water $S_\Delta \approx 0.30$ and $k_{31}(=k_q^T) \leq 5.0 \times 10^9$ M^{-1} s^{-1}. On the basis of $k_{31}(=k_q^T) \leq 5.0 \times 10^9$ M^{-1} s^{-1}, competition kinetics predict that in our experimental systems ^{3}CBP will directly react with DMS to the extent of ≥98% in system II (3.4×10^{-2} M DMS, 2.5×10^{-4} M O_2; air-saturated), ≥89% in system III (3.4×10^{-2} M DMS, 1.25×10^{-3} M O_2; oxygen-saturated), and ≥88% in system I (6.8×10^{-3} M DMS, 2.5×10^{-4} M O_2; air-saturated). From these calculations we conclude that direct oxidation of DMS by ^{3}CBP should produce the major fraction of sulfur radical cations, responsible for the *SOD-dependent* DMSO formation via reaction sequences 11, 13, 14 and 8 in systems I-III. Before a detailed consideration of the reaction mechanisms we shall summarize the evidence for the involvement of sulfur radical cations in the *SOD-dependent* sulfoxide formation. A comparison of DMS and DES reveals significantly smaller *SOD-dependent* but significantly higher *SOD-independent* sulfoxide yields for DES (see Table 4). The dimeric radical cation of DES ($[(CH_3CH_2)_2S\therefore S(CH_2CH_3)_2]^+$, **2b**) is less stable than the analogous species from DMS, **2a**, and suffers much faster deprotonation (via the monomer **1b**) (reactions 35 and 36).[13]

$$\mathbf{2b} \rightleftharpoons (CH_3CH_2)_2S^{\bullet+}\ (\mathbf{1b}) + (CH_3CH_2)_2S \qquad (35)$$

$$\mathbf{1b} \rightarrow H^+ + CH_3C^{\bullet}H\text{-}S\text{-}CH_2CH_3 \qquad (36)$$

Any potential reaction of superoxide with **2b** has to compete against deprotonation, and, therefore, sulfoxide formation via sulfur radical cations will be less efficient for DES as compared to DMS. The higher *SOD-independent* sulfoxide yields from DES (compared to DMS) then suggest that these do not directly originate from intermediary sulfur radical cations.

A second line of evidence for the involvement of **1a**/**2a** in the *SOD-dependent* formation of DMSO derives from the experiments in H_2O and D_2O. The experimentally observed product isotope effect of $[DMSO]_{H_2O}/[DMSO]_{D_2O} = 2.0$ correlates with the product isotope effect of $[\mathbf{2a}]_{H_2O}/[\mathbf{2a}]_{D_2O} = \Phi_{el,H_2O}/\Phi_{el,D_2O} = 1.7$, derived by laser photolysis.[10] The slight difference between 2.0 and 1.7 can be rationalized by additonal secondary (solvent) isotope effects on the formation of DMSO, i.e., a more efficient (competitive) reaction of DO^- as compared to HO^- [25] with intermediates **2a** and **10** (see also below).

2. The Potential Role of Hydrogen Peroxide for the *SOD-Independent* Pathway. A major contribution of hydrogen peroxide to the *SOD-independent* pathway can be excluded. For all our photolysis experiments any potential contribution of hydrogen peroxide was minimized by the addition of catalase immediately after irradiation (catalase cannot be present during the photoexperiment due to photolytic inactivation of the enzyme). Thus, catalase was present in the reaction mixtures at times ≤ 180 s after start of the photolysis (depending on the duration of photolysis which was generally between 0 and 100 s), limiting the reaction time for hydrogen peroxide and DMS to at most 180 s. An upper limit for the concentration of photolytically generated hydrogen peroxide concentrations can be obtained (representatively in H_2O) from the quantum efficiency of the CBP reduction. The combined yields of CBP

(24) Clennan, E. L.; Yang, K. *J. Org. Chem.* **1992**, *57*, 4477−4487.
(25) Schowen, R. L. *Prog. Phys. Org. Chem.* **1972**, *9*, 275−332.

reduction by DMS (via electron and hydrogen transfer) would amount to $-d[CBP]/dt = 1.22 \times 10^{-6}$ M s^{-1}. One-electron reduced CBP (species **7** or **7**$^-$) then produces superoxide (reactions 16 and 30) with $d[O_2^{\bullet-}]/dt = -d[CBP]/dt = 1.22 \times 10^{-6}$ M s^{-1}, which dismutates to hydrogen peroxide with $d[H_2O_2]/dt = 0.5\ (d[O_2^{\bullet-}]/dt) = 6.1 \times 10^{-7}$ M s^{-1}. The rate constant for the oxidation of DMS by hydrogen peroxide can be approximated as $k_{37} \approx 10^{-2}$ M^{-1} s^{-1}.[26]

$$H_2O_2 + {>}S \rightarrow H_2O + {>}S{=}O \qquad (37)$$

Equation (I), where $[H_2O_2]_0 = 6.1 \times 10^{-7}$ M s^{-1}, yields an upper limit for hydrogen peroxide-derived DMSO formation within 180 s of 7.4×10^{-9} M s^{-1} for 6.8×10^{-3} M DMS (system I) and 3.6×10^{-8} M s^{-1} for 3.4×10^{-2} M DMS (systems II and III).

$$[DMSO] = ([H_2O_2]_0 - [H_2O_2]) = [H_2O_2]_0(1 - e^{-k_{37}[DMS]t}) \qquad (I)$$

Both values are significantly lower than the experimentally obtained sulfoxide yields, even for the less efficient *SOD-independent* pathway. Thus, we can exclude hydrogen peroxide as a major source of DMSO formation under our experimental conditions.

Scheme 1

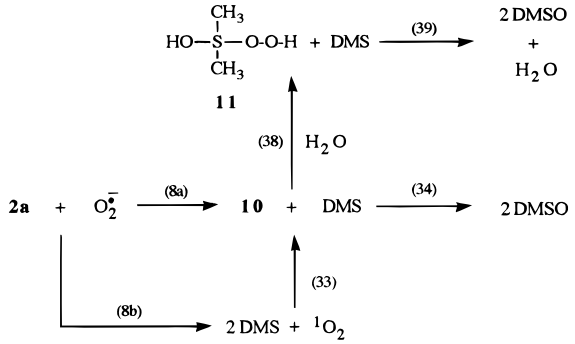

3. The Mechanism. A mechanism which rationalizes all our experimental findings includes the reactions displayed representatively for DMS in Scheme 1. On the *SOD-dependent* side, initially present dimeric sulfur radical cations **2a** react with superoxide anion to yield the zwitterionic structure **10** either via direct coupling of **2a** and **10** (reaction 8a) or via electron transfer (reaction 8b) followed by addition of singlet oxygen to DMS (reaction 33). Intermediate **10** either reacts directly with a second nonoxidized molecule of DMS (reaction 34)[1] or converts into the hydroperoxy sulfurane **11** (reaction 38) which may also oxidize DMS to generate 2 equiv of DMSO per equivalent of **11** (reaction 39). This mechanism shows little variation over the pH range 6.2−9.0. At pH > 9.0, hydroxide ions competitively react with **2a** and/or **10**, lowering the DMSO yields, where the reaction of hydroxide ion with **2a** yields intermediate(s) representing precursor(s) for *superoxide-independent* sulfoxide formation (see below). We note that besides the reaction of HO$^-$ with a "naked" radical cation **2a** (reaction 3) we have to consider the more general possibility of proton abstraction by HO$^-$ from a hydrated dimeric sulfur radical cation leading to **3** (reaction 40). Theoretical calculations have suggested that sulfur radical cations are present as hydrated forms where the bond dissociation energy of the $R_2S^{\bullet+}\cdots OH_2$ bond amounts to approximately 16.8 kcal/mol.[27]

$$HO^- + [(H_2O)_m\cdots{>}S\therefore S{<}]^+ \rightarrow mH_2O + \mathbf{3} \qquad (40)$$

On the *SOD-independent* side some DMSO originates from singlet oxygen (reaction 33 and 34; see below) and hydrogen peroxide (reaction 37). However, at pH > 9.0, the following intermediates have to be considered as major sources for a hydroxide-mediated sulfoxide formation: the monomeric hydroxy sulfuranyl radical **4**, its adduct with a second nonoxidized thioether **3**, and the methylthiomethylperoxyl radical **12** which forms via hydroxide-mediated deprotonation of **1a** (or **2a**) to yield the methylthiomethyl radical, followed by addition of molecular oxygen (reactions 21, 41, and 42).

$$\mathbf{1a} + HO^- \rightarrow {}^{\bullet}CH_2SCH_3 + H_2O \qquad (21)$$

$$\mathbf{2a} + HO^- \rightarrow (CH_3)_2S + {}^{\bullet}CH_2SCH_3 + H_2O \qquad (41)$$

$${}^{\bullet}CH_2SCH_3 + O_2 \rightarrow CH_3SCH_2OO^{\bullet}\ (\mathbf{12}) \qquad (42)$$

A defined concentration of **12** will always be present independent of reactions 21 and 41 since the hydrogen abstraction reaction 15 directly yields methylthiomethyl radicals. The following quantification shall primarily be based on results derived from the photolysis of system II, although crossreference will be made to the other systems I and III for specific information and control of the calculations.

4. The Quantitative Contribution of the Individual Processes to the *SOD-Independent* Sulfoxide Formation. In systems II and III, both containing 3.4×10^{-2} M DMS, maximal 3.6×10^{-8} M s^{-1} of the *SOD-independent* sulfoxide formation will result from the direct oxidation of DMS by hydrogen peroxide (reaction 37) (see above). The contribution of singlet oxygen to the *SOD-independent* sulfoxide formation can now be estimated from the difference of the *SOD-independent* sulfoxide yields at pH 6.2 of systems II and III (ΔDMSO-(III-II)$_{SOD-ind,pH\ 6.2}$). This difference $\Delta DMSO(III\text{-}II)_{SOD-ind,pH\ 6.2}$ should be due to different initial yields of $^1O_2$ in both systems since the yields of hydrogen peroxide and **12** should be essentially similar, only depending on the DMS concentration (determining photolytic conversion of CBP) and pH (determining hydroxide-catalyzed deprotonation of **1a** and **2a**). Moreover, the hydroxide-based processes such as deprotonation of **1a** and **2a** or formation of the adducts **3** and **4** are relatively inefficient at pH 6.2.[3] From equation II we calculate that the ratio of singlet oxygen formation in systems III and II, $R_{III/II}$, amounts to $R_{III/II} = 4.56$, where $k_{31} \leq 5 \times 10^9$ M^{-1} s^{-1} (see above), $k_9 = 1.5 \times 10^9$ M^{-1} s^{-1},[9] [DMS] $= 3.4 \times 10^{-2}$ M, and the oxygen concentrations in air-saturated and oxygen-saturated solution are $[O_2]_{air} = 2.5 \times 10^{-4}$ M and $[O_2]_{oxy} = 1.25 \times 10^{-3}$ M, respectively.

$$R_{III/II} = \frac{[^1O_2]_{III}}{[^1O_2]_{II}} = \frac{[O_2]_{oxy}}{[O_2]_{air}} \times \frac{k_{31}[O_2]_{air} + k_9[DMS]}{k_{31}[O_2]_{oxy} + k_9[DMS]} \qquad (II)$$

On the basis of literature values for the reaction of singlet oxygen with various thioethers[28] we approximate that $k_{33} \leq 1.0 \times 10^8$ M^{-1} s^{-1}, and, therefore, equation III predicts that singlet oxygen will nearly completely react with DMS when [DMS] $= 3.4 \times 10^{-2}$ M rather than suffer quenching by the solvent (reaction 43; $k_{43,H_2O} = 3.5 \times 10^5$ s^{-1} [32]).

$$[DMSO] = [^1O_2]_{total} \times \frac{k_{33}[DMS]}{k_{33}[DMS] + k_{43}} \qquad (III)$$

$$^1O_2 + H_2O \rightarrow {}^3O_2 + H_2O \qquad (43)$$

(26) Sysak, P. K.; Foote, C. S.; Ching, T.-Y. *Photochem. Photobiol.* **1977**, *26*, 19−27.

(27) Clark, T. in *Sulfur-Centered Reactive Intermediates in Chemistry and Biology*; Chatgilialoglu, C., Asmus, K.-D., Eds.; NATO ASI Series: Plenum Press: New York, 1990; Vol. 197, 13−18.

With $\Delta DMSO(III\text{-}II)_{SOD-ind,pH\ 6.2} = 7 \times 10^{-8}$ M s^{-1}, a stoichiometry of 2 equiv of sulfoxide per equivalent of singlet oxygen, and $R_{III/II} = 4.56$ we calculate that the initial yields of singlet oxygen in system II should be on the order of $[^1O_2]_{II} \approx 0.77 \times 10^{-8}$ M s^{-1}. This initial yield corresponds well to a theoretical value of $[^1O_2]_{II} \leq 1.5 \times 10^{-8}$ M s^{-1}, predicted according to equation IV on the basis of a competitive reaction of ^{3}CBP with DMS and $^3O_2$.

$$[^1O_2] \leq [^3CBP]S_\Delta \times \frac{k_{31}[O_2]}{k_{31}[O_2] + k_9[DMS]} \qquad (IV)$$

With $[^1O_2]_{II} \approx 0.77 \times 10^{-8}$ M s^{-1}, the singlet oxygen-derived DMSO yields in system II are on the order of 1.54×10^{-8} M s^{-1}. Subtraction of the hydrogen peroxide- and singlet oxygen-derived yields from the total *SOD-independent* sulfoxide yield at pH 6.2, 1.30×10^{-7} M s^{-1}, leaves 7.8×10^{-8} M s^{-1} for DMSO formation through pathways other than involving hydrogen peroxide and singlet oxygen. These reactions likely involve **12**, the adducts **3** and **4**, and, though speculative at present, eventually a reaction of **2a** with hydrogen peroxide. We note an increase of the *SOD-independent* sulfoxide yields with increasing pH between pH 6.2 and 9.0. Since hydrogen peroxide and singlet oxygen are not expected to show any significant pH-dependent variation of reactivity toward DMS in this pH region,[26] the pH-dependent increasing yields of DMSO may be rationalized by a pH-dependent reactivity of **3**, **4**, **12**, and/or **2a** (besides the addition of HO^-).

5. Sulfoxide Formation at pH > 9.0. There is a significant drop of the *SOD-dependent* sulfoxide yields at pH > 9.0 whereas the *SOD-independent* sulfoxide yields still increase. In system II, this decrease of 1.2×10^{-7} M s^{-1} of the *SOD-dependent* DMSO yields between pH 9.0 and 10.0 is paralleled only by a 1.4×10^{-8} M s^{-1} increase of the *SOD-independent* DMSO yields, indicating that a potential reaction of HO^- with **2a** leads to intermediates which yield sulfoxide less efficiently.

For mechanistic considerations we shall first discuss the formation of DMS^{18}O in $^{16}O_2/H_2{}^{18}O$ systems, pH 10 (Table 3, entries 4 and 5), which yields information as to which species contribute to the decreasing DMSO yields between pH 9 and 10.

Several pathways are possible: (i) An addition of hydroxide ion to the electrophilic sulfur of **10** initially yields a hydroperoxysulfurane anion (reaction 44). According to a proposal by Sysak et al.,[26] the latter may eliminate hydrogen peroxide to yield sulfoxide (reaction 45).

$$H^{18}O^- + >S^{(+)}\text{-}{}^{16}O\text{-}{}^{16}O^{(-)} \rightarrow H^{18}O\text{-}S(CH_3)_2\text{-}{}^{16}O\text{-}{}^{16}O^- \qquad (44)$$

$$H^{18}O\text{-}S(CH_3)_2\text{-}{}^{16}O\text{-}{}^{16}O^- + H^+ \rightarrow {}^{18}O{=}S< + H_2{}^{16}O_2 \qquad (45)$$

Based on the effect of pH on the singlet oxygen-mediated sulfoxide yields of *N*-formylmethionine amide,[26] we expect the reaction of hydroxide with **10** to be responsible for an 11% reduction of the DMSO yields on going from pH 9 to pH 10. Considering that reactions 44 and 45 lead to 1 equiv of DMS^{18}O per equivalent of **10**, an 11% reduction of the SOD-dependent yields is consistent with a fraction of 22% of **10** decomposing via reactions 44 and 45, and 78% of **10** decomposing via reaction 34. With the *SOD-dependent* DMSO yields accounting for ca. 2/3 of the total DMSO yields, and the SOD-independent pathway contributing a fraction of 5.9% of DMS^{18}O (entry 5, Table 3), we derive that such reaction should yield total DMSO yields of which a fraction of 10.2% contains ^{18}O. Experimentally we observed a fraction of 2.63% (Table 3, entry 5), demonstrating that reaction sequence 44 and 45 alone is unlikely to cause the hydroxide mediated reduction of the DMSO yields. (ii) Alternatively, hydroxide ion could attack species **10** on the terminal oxygen which, according to a suggestion of Foote and co-workers for protic solvents,[33] should accept protons from water (reaction 46). Such a mechanism could account for a hydroxide-mediated reduction of the DMSO yields without any significant incorporation of ^{18}O into DMSO.

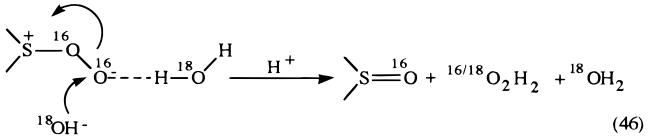

(46)

(iii) If reaction 44 were not followed by the elimination of hydrogen peroxide, a direct oxidation of of a second molecule DMS could occur (reactions 47 and 48).

$$H^{18}O\text{-}S(CH_3)_2\text{-}{}^{16}O\text{-}{}^{16}O^- + >S \rightarrow {}^{16}O{=}S< + H^{18}O\text{-}S(CH_3)_2\text{-}{}^{16}O^- \qquad (47)$$

$$H^{18}O\text{-}S(CH_3)_2\text{-}{}^{16}O^- \rightarrow {}^{16/18}OH^- + {}^{16/18}O{=}S< \qquad (48)$$

However, since reaction sequence 47 and 48, like species **10**, yields 2 equiv of DMSO, such reaction of hydroperoxy sulfurane intermediates would not lead to a pH-dependent reduction of the DMSO yields unless the hydroperoxy sulfurane reacts via additional competitive pathways which yield less or no sulfoxide. The possibility of sulfone formation (reaction 49)[24] can be excluded since sulfone yields in our systems were generally low (see Table 4).

$$HO\text{-}S(CH_3)_2\text{-}O\text{-}O^- \rightarrow HO^- + (CH_3)_2SO_2 \qquad (49)$$

(iv) An alternative would be the reaction of hydroxide ion with the hydroperoxysulfurane (reaction 50), followed by reaction 48.

$$H^{18}O\text{-}S(CH_3)_2\text{-}{}^{16}O\text{-}{}^{16}OH + {}^{18}OH^- \rightarrow H_2{}^{16/18}O_2 + H^{18}O\text{-}S(CH_3)_2\text{-}{}^{16}O^- \qquad (50)$$

Analogous to the calculations above, this pathway would lead to an overall incorporation of ca. 5.1% ^{18}O into the total DMSO yields, a value, though closer, still higher than experimentally determined for DMSO formation in the absence of SOD (2.63%). Thus, at present reaction 46 represents the most probable mechanism based on the incorporation of ^{18}O and the overall yield of DMSO. However, we cannot exclude that at

(28) There are several examples showing that the rate constants for the reaction of $^1O_2$ with sulfides are quite similar in solvents of different polarity, e.g. for $(i\text{-}C_3H_7)_2S$, $k = 2.5 \times 10^6$ M^{-1} s^{-1} in CH_3OH[29] and $k = 2.2 \times 10^6$ M^{-1} s^{-1} in $CHCl_3$,[30] for $(t\text{-}C_4H_9)_2S$, $k = 1.5 \times 10^5$ M^{-1} s^{-1} in CH_3OH[29] and $k = 1.3 \times 10^5$ M^{-1} s^{-1} in $CHCl_3$,[30] and for methionine, $k = 8.6 \times 10^6$ M^{-1} s^{-1} in H_2O[31] and $k = 1.4 \times 10^7$ M^{-1} s^{-1} (for the CBZ-L-methionine methyl ester) in $CHCl_3$.[30] Furthermore, it was shown that, although important for sulfides with branched substituents (see above), steric effects appear to be less significant for *n*-alkyl substituted sulfides, e.g. compare the rate constants for $(n\text{-}C_4H_9)_2S$ and $n\text{-}C_4H_9SCH_3$ in $CHCl_3$ which are 2.3×10^7 and 2.9×10^7 M^{-1} s^{-1}, respectively.[30] The oxidation of $(C_2H_5)_2S$ by $^1O_2$ in methanol occurs with $k = 1.7 \times 10^7$ M^{-1} s^{-1}.[29] Thus, an upper limit for the oxidation of DMS by $^1O_2$ in water may be set at $k \leq 1.0 \times 10^8$ M^{-1} s^{-1}.

(29) Kacher, M. L.; Foote, C. S. *Photochem. Photobiol.* **1979**, *29*, 765−769.
(30) Monroe, B. M. *Photochem. Photobiol.* **1979**, *29*, 761−764.
(31) Kraljic, I.; Sharpatyi, V. A. *Photochem. Photobiol.* **1978**, *28*, 583−586.
(32) Merkel, P. B.; Kearns, D. R. *J. Am. Chem. Soc.* **1972**, *94*, 1029−1030.
(33) Gu, C.; Foote, C. S.; Kacher, M. L. *J. Am. Chem. Soc.* **1981**, *103*, 5949−5951.

least part of the reaction of hydroxide with **10** proceeds through reactions 47, 48, and 50.

In this respect, we note that the SOD-*independent* DMSO formation shows higher levels of ^{18}O incorporation (5.9%) than the total DMSO formation (2.63%). Thus, very likely the mechanism leading to the incorporation of ^{18}O into DMSO does not at all involve intermediate **10**. Given that the hydroxide pathway via species **5**, or the analogous species HO-S$(CH_3)_2$-S$(CH_3)_2$-OO$^\bullet$ (**13**), a potential intermediate during reaction 5,[3] leads to incorporation of the water oxygen into DMSO,[3] we derive that at most 1.8×10^{-8} M s^{-1} of the *SOD-independent* DMSO yields at pH 10 can originate from reactions 3−7. This fraction of 1.8×10^{-8} M s^{-1} is close to the observed increase of the *SOD-independent* DMSO yields on going from pH 9.0 to 10.0 (1.4×10^{-8} M s^{-1}) and may reflect the hydroxide pathway (intermediates **5** and/or **13**) as an additional competitive pathway reducing the DMSO yields at pH 10. From these considerations it becomes clear that **5** and **13** (as well as hydrogen peroxide and singlet oxygen) are not major contributing species to the SOD-*independent* sulfoxide formation in this pH region. However, it appears that the *hydroxide pathway* (reactions 3−7) is responsible for the experimentally observed incorporation of ^{18}O into DMSO, a conclusion supported by solvent isotope effects (see below).

The majority of the *SOD-independent* DMSO must, therefore, originate from other species, e.g., the peroxyl radical **12**. Peroxyl radicals are known to oxidize sulfides, and such reactions will become particularly important at the high DMS concentration of 3.4×10^{-2} M (i.e., at low [DMS] = 1.0×10^{-3} M, **12** did not significantly oxidize DMS[3]). A potential mechanism would involve an oxygen transfer reaction between **12** and a second sulfide (reaction 51) since the source of oxygen has to be molecular oxygen, present through addition of O_2 at $^\bullet CH_2SCH_3$. The resulting oxyl radical will react via fragmentation (reaction 52), rearrangement (reaction 54), or hydrogen abstraction from a second sulfide (reaction 55). Reactions 54 and 55 appear, however, less probable based on the expected poor stability of $CH_3SCH_2O^\bullet$ with regard to fragmentation reaction 52.

$$\mathbf{12} + \text{S<} \rightarrow CH_3SCH_2O^\bullet + \text{>S=O} \quad (51)$$

$$CH_3SCH_2O^\bullet \rightarrow CH_3S^\bullet + CH_2O \quad (52)$$

$$2CH_3S^\bullet \rightarrow CH_3SSCH_3 \quad (53)$$

$$CH_3SCH_2O^\bullet \rightarrow CH_3\text{-}S\text{-}{}^\bullet CH\text{-}OH \quad (54)$$

$$CH_3SCH_2O^\bullet + \text{S<} \rightarrow CH_3SCH_2OH + {}^\bullet CH_2SCH_3 \quad (55)$$

6. The Rate Constant k_8. The rate constant k_8 ($=k_{8a} + k_{8b}$) can be determined from the plot displayed in Figure 3, reflecting the competitive reaction of superoxide with the SOD dimer (reactions 56 and 57), or with radical cation **2a** (reaction 8), respectively.

$$\mathbf{2a} + O_2^{\bullet-} \rightarrow \mathbf{10} + \text{DMS} \rightarrow (\text{DMSO} + \text{products}) \quad (8)$$

$$O_2^{\bullet-} + \text{SOD} \rightarrow \text{SOD}_{red} \quad (56)$$

$$O_2^{\bullet-} + \text{SOD}_{red} + 2H^+ \rightarrow H_2O_2 \quad (57)$$

The steady-state concentrations of radical cation **2a**, $[\mathbf{2a}]_s$, and superoxide, $[O_2^{\bullet-}]_s$, are derived from equations (V)-(VIII).

$$\frac{d[\mathbf{2a}]}{dt} = \Phi_{el}[^3CBP] - k_3[HO^-][\mathbf{2a}] - k_8[\mathbf{2a}][O_2^{\bullet-}] \quad (V)$$

For $d[\mathbf{2a}]/dt = 0$ equation (VI) follows.

$$[\mathbf{2a}]_s = \frac{\Phi_{el}[^3CBP]}{k_3[HO^-] + k_8[O_2^{\bullet-}]_s} \quad (VI)$$

The calculation of $[O_2^{\bullet-}]_s$ is based on the fact that each dismutation of superoxide by SOD consumes 2 equiv of superoxide and that k_{56} is rate-determining,[34] with $k_{56} = 2.0 \times 10^9$ M^{-1} s^{-1} for superoxide concentrations between 10^{-13} and 5.0×10^{-5} M.[34] We note that in the presence of SOD we do not have to include a term of uncatalyzed dismutation of superoxide (reaction 58) since its rate is negligible compared to the reaction of superoxide with SOD.[19]

$$2O_2^{\bullet-} + 2H^+ \rightarrow H_2O_2 \quad (58)$$

Equations VII and, for $d[O_2^{\bullet-}]/dt = 0$, VIII follow where the initial yield of $O_2^{\bullet-}$ is determined by the initial yield of **7** and **7**$^-$, $(\Phi_{el} + \Phi_H)[^3CBP]$, on the basis of reactions 13−16 and 30.

$$\frac{d[O_2^{\bullet-}]}{dt} = (\Phi_{el} + \Phi_H)[^3CBP] - k_8[\mathbf{2a}]_s[O_2^{\bullet-}] - 2k_{56}[SOD][O_2^{\bullet-}] \quad (VII)$$

$$[O_2^{\bullet-}]_s = \frac{(\Phi_{el} + \Phi_H)[^3CBP]}{k_8[\mathbf{2a}]_s[O_2^{\bullet-}] + 2k_{56}[SOD]} \quad (VIII)$$

Figure 3 shows that $[S{=}O]_{max}/[S{=}O] = 2.0$ at $[SOD] = 2.3 \times 10^{-9}$ M (for native SOD, $f_a = 1.0$). At this ratio we theoretically expect that $k_8[\mathbf{2a}] = 2k_{56}[SOD] = 9.2$ where $k_{56} = 2.0 \times 10^9$ M^{-1} s^{-1}.[34] With $k_8[\mathbf{2a}] = 9.2$, $\Phi_{el} = 0.17$, $\Phi_H = 0.12$, and $[^3CBP] = 4.2 \times 10^{-6}$ M s^{-1} (see above), equation VIII yields $[O_2^{\bullet-}]_s = 6.6 \times 10^{-8}$ M for $[SOD] = 2.3 \times 10^{-9}$ M. Rearrangement of equation VIII leads to equation IX which yields $k_8 = 2.3 \times 10^{11}$ M^{-1} s^{-1} where $k_3 = 2.6 \times 10^9$ M^{-1} s^{-1} [35] and $[HO^-] = 1 \times 10^{-6}$ M.

$$k_8 = \frac{k_3[HO^-]}{[O_2^{\bullet-}]_s\Phi_{el}[^3CBP]} \times \left[\frac{1}{(\Phi_{el} + \Phi_H)[^3CBP] - 2k_{56}[O_2^{\bullet-}]_s[SOD]} - \frac{1}{\Phi_{el}[^3CBP]}\right]^{-1} \quad (IX)$$

This value for k_8 should be given with at least ±50% error, i.e., $k_8 = (2.3 \pm 1.2) \times 10^{11}$ M^{-1} s^{-1}, in the light of possible errors of 10−20% each in the determination of ^{3}[CBP], k_3, and $[O_2^{\bullet-}]_s$. Nevertheless, the reaction of superoxide with **2a** occurs with a very high rate constant, comparable to the neutralization of hydroxide ions by protons.[36] This high rate constant may actually reflect that the electron transfer process (reaction 8b) predominates over the radical−radical coupling of superoxide with **2a** (reaction 8a).

(34) (a) Klug, D.; Rabani, J.; Fridovich, I. *J. Biol. Chem.* **1972**, *247*, 4839−4842. (b) Rotilio, G.; Bray, R. C.; Fielden, M. *Biochim. Biophys. Acta* **1972**, *268*, 605−609. (c) Forman, H. J.; Fridovich, I. *Arch. Biochem. Biophys.* **1973**, *158*, 396−400.

(35) By analogy to the reaction of hydroxide ion with the intramolecular three-electron bonded sulfur radical cation of the peptide cyclo-Met-Met. Holcman, J.; Bobrowski, K.; Schöneich, Ch.; Asmus, K.-D. *Radiat. Phys. Chem.* **1991**, *37*, 473−478.

(36) Eigen, M.; De Maeyer, L. *Z. Elektrochem.* **1955**, *59*, 986.

7. The Competition of Hydroxide Ion and Superoxide for 2a. We can now derive an estimate for the competition of hydroxide ion and superoxide for **2a** at pH 10. For this treatment we need the steady-state concentration of superoxide ion in the absence of SOD. In a first approximation the initial yield of superoxide, equal to $(\Phi_{el} + \Phi_H)$ [^{3}CBP], will be reduced by the fast reaction of superoxide with radical cation **2a** of an initial yield Φ_{el} [^{3}CBP] (reaction 8). A residual amount of superoxide, equal to Φ_H [^{3}CBP], remains available for reactions 58 and 59.

$$CH_3SCH_2OO^{\bullet}\ (\mathbf{12}) + O_2^{\bullet -} \rightarrow \text{products} \qquad (59)$$

We cannot derive the steady state concentration of **12** and k_{59} is not known. Neglecting reaction 59 in a first approximation enables us to use equations X and XI to obtain $[O_2^{\bullet -}]_s \leq 2.9 \times 10^{-5}$ M in the absence of SOD where the observed rate constant for reaction 58 at pH 10 is $k_{58,pH10} = 6 \times 10^2\ M^{-1}\ s^{-1}$.[19]

$$\frac{d[O_2^{\bullet -}]}{dt} \leq \Phi_H[^3CBP] - k_{58}[O_2^{\bullet -}]^2 \qquad (X)$$

$$[O_2^{\bullet -}]_s \leq \sqrt{\frac{\Phi_H[^3CBP]}{k_{58}}} \qquad (XI)$$

The application of equation XII then predicts that an increase from pH 9 to pH 10 in system II should reduce the efficiency of reaction 8, f_8, to an extent of ca. 5% based on a competition of superoxide and HO^- for **2a**.

$$f_8 \approx \frac{k_8[O_2^{\bullet -}]_s}{k_8[O_2^{\bullet -}]_s + k_3[HO^-]} \qquad (XII)$$

Together with the additional 11% reduction of the sulfoxide yields through reaction of hydroxide ion with **10**[26] (see above), the combined action of hydroxide on **10** and, competitively with superoxide, on **2a** is expected to reduce the *SOD-dependent* DMSO yields by ca. 16% on going from pH 9 to 10.

Experimentally, we observe that the *SOD-dependent* DMSO yields in system II decrease by 16.5% when the pH is increased from 9.0 to 10.0. Thus, the experimental and theoretically predicted yields are correlating well, supporting the quantitative analysis of our proposed reaction mechanism.

8. Solvent Isotope Effects. The effect of H_2O/D_2O on the *SOD-dependent* DMSO yields has been rationalized by the different yields of **2a** in both solvents. For the *SOD-independent* DMSO yields the product isotope effects clearly support the conclusion that singlet oxygen is not a major source of DMSO. In particular at [DMS] = 6.8×10^{-3} M we would have expected higher DMSO yields in D_2O due to the increased lifetime of $^1O_2$ in D_2O.[37] Instead, we observe nearly similar *SOD-independent* DMSO yields in H_2O and D_2O for [DMS] $\leq 2.0 \times 10^{-2}$ M. Moreover, a normal solvent isotope effect of 1.58 is derived for [DMS] = 3.4×10^{-2} M. At high DMS concentrations the major process leading to the SOD-*independent* DMSO formation is reaction 51 (see above). On the basis of the highly dipolar structure of DMSO we believe that the oxygen transfer process is associated with solvation and hydrogen bonding of the developing DMSO molecule as displayed in the transition structure **14**.

Thus, in the course of reaction 51 protons of solvent water molecules will change their fractionation factors of $\Phi = 1.0$ to

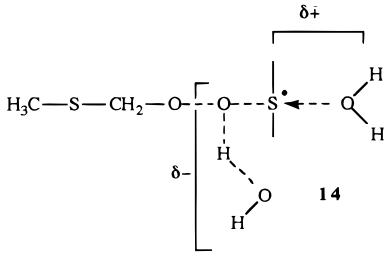

fractionation factors $\Phi < 1.0$ in the transition state (structure **14**).[25,38] Since reaction 51 does not contain any (rate determining) proton transfer step, this situation is consistent with an overall normal solvent isotope effect based on relation XIII (R = reactant sites; TS = transition state sites).

$$\frac{k_H}{k_D} = \frac{\prod_i \Phi_i^R}{\prod_j \Phi_j^{TS}} \qquad (XIII)$$

The peroxyl radical **12** alone may exist in a weakly dipolar structure (associated with some hydrogen bonding to the surrounding water). But this hydrogen bonding should become even stronger in the transition structure **14**, consistent with an overall normal solvent isotope effect.

The comparison of entries 6 and 7 in Table 3 reveals that there is a significantly higher incorporation of ^{18}O into DMSO when the reaction was carried out in $H_2{}^{18}O/D_2{}^{16}O$ (1:1, v/v) instead of $H_2{}^{18}O/H_2{}^{16}O$ (1:1, v/v) with an inverse product isotope effect of 2.50 for the *SOD-independent* pathway. Such an inverse isotope effect is consistent with the contribution of an equilibrium isotope effect involving several protons with fractionation factors of the reactant state of $\Phi^R < 1.0$ and product state fractionation factors $\Phi^P \approx 1.0$.[38] We can neglect any contribution of a reaction of lyoxide (LO^-; L = H, D) with **10** to this observed isotope effect since **10** does not form in significant amounts in the presence of SOD. Thus, this isotope effect can be rationalized by a reaction of lyoxide with **2a** and subsequent reactions. In equilibrium 60 lyoxide reacts with a hydrated species **2a** to yield L_2O and **3** (which is in equilibrium with **4**).

$$LO^- + [(L_2O)_m \cdots > S \therefore S <]^+ \rightleftharpoons m L_2O + LO\text{-}S(CH_3)_2\text{-}(H_3C)_2S^{\bullet}\ (\mathbf{3}) \qquad (60)$$

The fractionation factors[25] of the protons of the hydrating water will depend on the partial positive charge x on the hydrating water molecule. We expect that with more than one water molecule involved in the hydration of **2a**, a higher average positive partial charge will reside on the hydrating water molecules, i.e., the value x will approach $x = 1/m$. The application of the Gross−Butler equation results in equation XIV where $\Phi_1{}^R = 0.5$, $\Phi_2{}^R = 0.69$, $\Phi_1{}^P = 1.0$, $\Phi_2{}^P = 1.0$, and $n = 0.5$ (atom fraction deuterium; $[H_2{}^{18}O]/[D_2{}^{16}O] = 0.5$).

$$K_{D,60} = K_{H,60} \frac{(1 - n + n\Phi_1{}^P)(1 - n + n\Phi_2{}^P)}{(1 - n + n\Phi_1{}^R)(1 - n + n[\Phi_2{}^R]^{1/m})^{2m}} \qquad (XIV)$$

For a reasonable average of three hydrating water molecules ($m = 3$) we can assume that $x \approx 0.33$, resulting in $K_{D,60}/K_{H,60} = 1.90$. In order to predict the complete solvent isotope effect

(37) (a) Merkel, P. B.; Nilsson, R.; Kearns, D. R. *J. Am. Chem. Soc.* **1972**, *94*, 1030−1031. (b)Merkel, P. B.; Kearns, D. R. *J. Am. Chem. Soc.* **1972**, *94*, 7244−7253.

(38) Schowen, K. B. J. In *Transition States of Biochemical Processes*; Gandour, R. D., Schowen, R. L., Eds.; Plenum Press: New York, 1978, 225−283.

for lyoxide-mediated sulfoxide formation, we have now to consider subsequent reactions of the intermediate **5**. This intermediate **5** should be relatively stable (as experimentally shown for the analogous intermediate from 2-methylthiomethyl acetate[5]). Equilibrium 61 will then be important for sulfoxide formation with the deprotonated species $\mathbf{5}^-$ being more reactive with respect to superoxide extrusion than the protonated species **5** which likely enters several competitive reaction pathways such as, e.g., reactions 62 and 63.

$$LO^- + LO\text{-}S(CH_3)_2OO^\bullet\ (\mathbf{5}) \rightleftharpoons L_2O + {}^-O\text{-}S(CH_3)_2OO^\bullet\ (\mathbf{5}^-) \quad (61)$$

$$2LO(CH_3)_2S\text{-}OO^\bullet \rightarrow O_2 + 2LO(CH_3)_2S\text{-}O^\bullet \quad (62)$$

$$LO\text{-}S(CH_3)_2O^\bullet \rightarrow CH_3SO_2^- + L^+ + {}^\bullet CH_3 \quad (63)$$

Because of the relative long lifetime of **5** (and $\mathbf{5}^-$),[5] equilibrium 61 shall be rapid compared to reaction 7. Thus, no primary isotope effect will result from the proton transfer but rather an equilibrium isotope effect. For equilibrium 61 the solvent isotope effect is given by equation XV where $\Phi_1{}^R = 0.5$ and $n = 0.5$ (assuming $\phi_{5^-} \approx 1.0$).

$$K_{D,61} = K_{H,61}\frac{1}{(1 - n + n\Phi_1{}^R)} = 1.33 \quad \text{(XV)}$$

The combination of both isotope effects yields $(K_D/K_H)_{total} = (K_{D,60}/K_{H,60})\ (K_{D,61}/K_{H,61}) = 2.53$, corresponding well to our experimentally observed isotope effect of 2.50.

9. Material Balance. In order to avoid secondary reactions of primary oxidants (^{3}CBP) with oxidation products, our experimental system was based on very low conversion of excess substrate, i.e., a photolytic conversion of $<2.0 \times 10^{-4}$ M DMS of an initial concentration of $\geq 6.8 \times 10^{-3}$ M. Thus, within experimental error we cannot directly measure the consumption of DMS and compare this value with the product yields. However, based on the known quantum yields of DMS oxidation by ^{3}CBP, the known (see above) initial photolytic production of ^{3}CBP, and the quantitative analysis of reaction products, a material balance can be obtained. Between pH 6.2 and 9.0 (system II), the oxidation of DMS by ^{3}CBP generates **12** with $\Phi_H[^3\text{CBP}] = 5.04 \times 10^{-7}$ M s^{-1} (reactions 15 and 51). Reactions 51−53 imply a stoichiometry of one molecule formaldehyde per molecule **12** so that about 5.04×10^{-7} M s^{-1} of the total observed formaldehyde yields (7.3×10^{-7} M s^{-1}) can be accounted for by the initial reaction 15. This leaves a residual amount of $\Delta_{H_2CO} = 2.26 \times 10^{-7}$ M s^{-1} of formaldehyde representative for other pathways. Between pH 6.2 and 9.0 an average of 1.02×10^{-6} M s^{-1} of DMSO is formed via the *SOD-dependent* pathway which has a stoichiometry of 2 molecules of DMSO per intermediate **10**, i.e., per **2a**. Thus, a fraction of 0.51×10^{-6} M s^{-1} **2a** forms *SOD-dependent* DMSO. However, **2a** is generated with $\Phi_{el}[^3\text{CBP}] = 7.14 \times 10^{-7}$ M s^{-1}, so that the difference between $\Phi_{el}[^3\text{CBP}]$ and 0.51×10^{-6} M s^{-1} **2a**, a residual yield of $\Delta_{2a} = 2.04 \times 10^{-7}$ M s^{-1}, reacts through other pathways. As discussed above a small fraction of Δ_{2a} will form SOD-*independent* DMSO yields via the hydroxide pathway (at pH 6.2−9.0 less than 6%) whereas the majority of Δ_{2a} will suffer deprotonation to yield ${}^\bullet CH_2SCH_3$ (reaction 21), available for formaldehyde production via **12** and subsequent reactions (including sulfoxide formation via reaction 51). In this respect $\Delta_{2a} = 2.04 \times 10^{-7}$ M s^{-1} correlates well with $\Delta_{H_2CO} = 2.26 \times 10^{-7}$ M s^{-1}. Reactions 51−53 demonstrate that $CH_3S^\bullet$ and CH_3SH are characteristic byproducts en route to formaldehyde. Table 4 displays that, at pH 6.5, the combined yield of CH_3SH, CH_3SSCH_3 (representing the initial formation of two $CH_3S^\bullet$) and CH_3SO_3H (4.0×10^{-7} M s^{-1}) is well on the order of the observed formaldehyde yields (among the missing products possibly being CH_3SO_2H). The latter were obtained for system III but should be quite similar to the ones obtained in system II, based on the general similarity of both systems with respect to the product yields (see Figure 1). Thus, our product quantities correlate well with the initial photolytic yields of ^{3}CBP, permitting a full quantitative analysis of our experimental system.

10. Conclusion. In the present work we have quantified several pathways which lead to the conversion of aliphatic sulfur radical cations to sulfoxide in aqueous solution. Clearly, superoxide can react with sulfur radical cation complexes to produce 2 equiv of sulfoxide per equivalent of one-electron oxidized sulfur. An important parameter is the stability of such sulfur radical cation complexes which slows down competing reaction pathways such as deprotonation reactions. In this respect we shall note that $[R_2S\therefore SR_2]^+$ radical cation complexes are, for example, observable when the dipeptide L-Met-L-Met is subjected to one-electron oxidation by hydroxyl radicals[39] or ^{3}CBP.[40] Preliminary experiments with L-Met-L-Met demonstrate that significant yields of the disulfoxide L-Met(O)-L-Met(O) are formed by reaction of superoxide with one-electron oxidized L-Met-L-Met.[41] Such pathway may be highly biologically relevant for the intracellular protein calmodulin. When isolated from aged brain, calmodulin contains significant amounts of methionine sulfoxide on the subsequence $Met_{71}-Met_{72}$[42] which can be rationalized by the involvement of reactive oxygen species (including superoxide) in age-related protein modifications.

Experimental Section

See Supporting Information.

Acknowledgment. This work was supported by a Allen and Lila Self Fellowship (to B.L.M.) and NIH (PO1AG12993-01). We wish to thank Mr. Robert Drake for his efforts in acquiring the GC-MS data, and we would like to express our thanks to one reviewer for valuable suggestions on the chemistry of intermediate **10** in aqueous solution.

Supporting Information Available: Experimental section (4 pages). See any current masthead page for ordering and Internet access instructions.

JA962032L

(39) Bobrowski, K.; Holcman, J. *J. Phys. Chem.* **1989**, *93*, 6381−6387.
(40) Hug, G. L.; Marciniak, B.; Bobrowski, K. *J. Photochem. Photobiol. A* **1996**, *95*, 81−88.
(41) Schöneich, Ch.; Zhao, F.; Yang, J.; Miller, B. L. In *Stability, Formulation and Delivery of Peptide and Proteins*; American Chemical Society Symposium Series **1996**, in press.
(42) Michaelis, M. L.; Bigelow, D. J.; Schöneich, Ch.; Williams, T. D.; Ramonda, L.; Yin, D.; Hühmer, A. F. R.; Yao, Y.; Gao, J.; Squier, T. C. *Life Sci.* **1996**, *59*, 405−412.